INTERNATIONAL JOURNAL FOR NUMERICAL METHODS IN FLUIDS
Int. J. Numer. Meth. Fluids **31**: 1311–1320 (1999)

SIMULATION OF THREE-DIMENSIONAL BUBBLES USING DESINGULARIZED BOUNDARY INTEGRAL METHOD

Y.L. ZHANG, K.S. YEO*, B.C. KHOO AND W.K. CHONG

Department of Mechanical and Production Engineering, National University of Singapore, Kent Ridge, Singapore 119260, Singapore

SUMMARY

A very simple model based on the three-dimensional desingularized boundary integral method is applied to study the evolution of bubble(s) with or without the presence of solid structures. The choice of the desingularization parameters, which is crucial to the success of the method, is studied in the context of bubble dynamics. With the proper choice of parameters, the new model is far more efficient than previous models with virtually the same level of accuracy being achieved. This is largely attributed to the simplicity of the desingularization method. Furthermore, the new model offers a simple and attractive way for mesh refinement. Although it has limitations in the sense that, with this model the time stepping tends to slow down as two surfaces approach each other, this can be easily rectified by switching over to a direct method so that the two surfaces can be drawn closer as required in the context of jet impact. After this the new model can be reinstated to treat the complicated doubly connected geometry involving toroidal bubbles that would otherwise be very difficult to deal with. Copyright © 1999 John Wiley & Sons, Ltd.

KEY WORDS: bubble dynamics; desingularized boundary integral method; three-dimensional

1. INTRODUCTION

One primary advantage of the boundary integral method (BIM) over other methods in the simulation of three-dimensional bubbles is that the dimensions of the problem are reduced by one, which greatly conserves the computational effort. Thus far, most of the three-dimensional computations for bubble dynamics have been carried out using the direct formulation in which both the potential and its normal derivative are involved in the integral equation [1]. One of the key issues in the implementation of the direct formulation is the accurate determination of material velocity on the discretized boundary, which is a non-smooth surface. A global or local surface interpolation scheme is usually needed to define the normal direction and tangential plane on the described surface. Harris [2] used an averaging of linear approximations on the surface element. However, this algorithm suffers from non-convergence under mesh refinement, as noted by Blake *et al.* [3]. Chahine *et al.* [4] used quadratic polynomials to fit the surface locally. However, as also noted by Blake *et al.* [3], the method fails for certain arrangements of the nodes and is thus not robust. Blake *et al.* [3] favoured the use of radial

* Correspondence to: Department of Mechanical and Production Engineering, National University of Singapore, Kent Ridge, Singapore 119260, Singapore. Tel: +65 8742246; fax: +65 7761962; e-mail: mpeyeoks@nus.edu.sg

CCC 0271–2091/99/241311–10$17.50
Copyright © 1999 John Wiley & Sons, Ltd.
Received August 1997
Revised December 1998

basis functions over other alternatives, since they were claimed to be universally applicable. However, as noted in a recent paper by the present authors [5], the interpolation scheme via radial basis functions is based on a bivariate representation $z=f(x, y)$ of the surface. As a result, a new orientation of Cartesian axes must be chosen once a part of the bubble surface becomes parallel to the z-axis (cf. Reference [3]). Recently, the authors [5] proposed the use of a trivariate interpolation scheme based on the nine-noded Lagrangian element. The trivariate representation is universal in that it can be applied anywhere on the bubble surface regardless of surface orientation. However, this approach may be cumbersome if mesh refinement is carried out as the bubble evolves or when the bubble undergoes topological changes from a singly connected region to a doubly connected region.

Indirect methods, in which the potential is represented as either single-layer (source distribution) or double-layer (dipole distribution) potential, have also been explored for both the axisymmetric and two-dimensional bubbles. Blake and Gibson [6] used a discrete ring source distribution to approximately represent the cavitation bubble and the adjacent free surface. Boulton-Stone [7] tried both source and dipole distribution methods. One of the advantages of the indirect methods over the direct methods is that the analytical form of the potential is obtained once the source/dipole density is found. However, this advantage is lost for the present problem since, when calculating the velocity the differentiation of the potential would give rise to some hyper–singular integrals, which cannot be interpreted in the sense of the Cauchy principal value. Boulton-Stone [7] got around this problem by using a quadratic fit of the bubble boundary. This, however, only seemingly removes the difficulty and results in a much smaller velocity once the singularity is smoothed out. In fact, it is reckoned that this was responsible for the abnormally early breakdown of this source method. Secondly, this also makes the said method less attractive as compared with the direct formulation, where the surface fitting is also required.

In the present paper, a desingularized indirect boundary integral method (DIBIM) is adapted to study three-dimensional bubbles. This method was proposed by Cao *et al.* [8] for general potential problems and was found to be advantageous over the conventional indirect methods both in terms of efficiency and accuracy, provided that some desingularization parameters are carefully chosen. With the proper choice of these parameters, we show that DIBIM is a powerful tool for the simulation of the interaction between bubbles and solid structures. As a result of the simplicity of the algorithm, the computational time and storage requirements are greatly reduced. More importantly, it can easily incorporate a mesh refinement scheme and may be extended to bubbles undergoing topological changes from a singly connected region to a doubly connected region. The last problem is not considered in the present paper. However, this method has the limitations near bubble distortion and the final phase of jet impact, and for this we propose a remedy of switching back to a direct method at an appropriate point of time. Maximum numerical efficiency can be achieved in this way.

2. THE DESINGULARIZED INDIRECT BOUNDARY INTEGRAL METHOD

For large-scaled bubbles (millimetre or larger) considered in this paper, the effect of surface tension is insignificant during most of the bubble's lifetime and is thus neglected here [9]. For small-scaled bubbles, surface tension can be very important throughout almost all of the bubble's lifetime and for this case, the following formulation must be modified to accommodate this effect. For potential flows, there exists a potential function $\phi(x, y, z, t)$ in the fluid region bounded by some bubbles and solid structures. A rectangular co-ordinate system

Copyright © 1999 John Wiley & Sons, Ltd.

(x, y, z) is adopted with the z-axis pointing vertically upwards (Figure 1). For brevity, only cavitation bubbles are considered in this paper, although the extension to gas-filled bubbles is straightforward. For the purpose of non-dimensionalization, R_m (the maximum bubble radius) and $R_m\sqrt{\rho/(p_\infty - p_c)}$ are chosen to be the length and time scales respectively, where p_∞ is the ambient pressure on the plane $z = \gamma$, which passes through the centre of the bubble at inception, and p_c is the constant pressure inside the bubble. Then the non-dimensionalized evolution equations can be written in a Lagrangian sense as

$$\frac{D\mathbf{r}}{Dt} = \nabla\phi, \tag{1}$$

$$\frac{D\phi}{Dt} = 1 + \frac{1}{2}|\nabla\phi|^2 - \delta^2(z - \gamma), \quad \text{on the bubble surface,} \tag{2}$$

where $\mathbf{r} = (x, y, z)$ and $\delta = [\rho g R_m/(p_\infty - p_c)]^{1/2}$ is the buoyancy parameter, and the bubble centre at inception is located at $(0, 0, \gamma)$. The initial conditions are derived by integrating the Rayleigh–Plesset equation from the time of inception to the time when the bubble growth is arrested. For cavitation bubbles, the initial value of the potential on the bubble, whose radius is assumed to be $\frac{1}{10}$ of the maximum radius, is given by (cf. Reference [10])

$$\phi(t_0) = -2.58, \quad \text{at } t_0 = 0.0015527. \tag{3}$$

The boundary conditions on the solid structure are given by

$$\frac{\partial\phi}{\partial n} = 0, \tag{4}$$

where n is the normal direction of the solid boundary.

In line with the indirect boundary integral method (IBIM) [1], the following single-layer potential is introduced:

$$\phi(P) = \int_S \frac{\sigma(Q)}{|P - Q|}\,dS(Q), \tag{5}$$

where σ is the unknown source density, $|P - Q|$ is the Euclidean distance between the control point P and the integration point Q. However, unlike the conventional IBIM, the integration surface S here is not the physical boundary but a fictitious surface located outside the problem

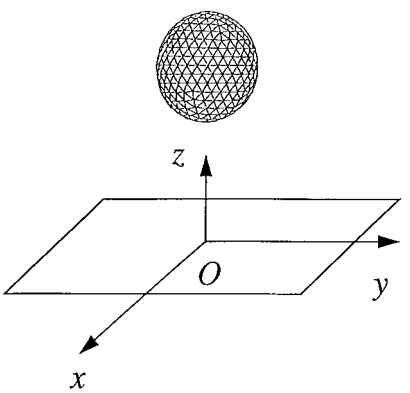

Figure 1. A definition sketch of a bubble near a solid wall and the co-ordinate system used.

Copyright © 1999 John Wiley & Sons, Ltd.

domain [8]. This process of desingularization renders the integral (5) non-singular and the integration can be replaced by a summation of concentrated singularities $\sigma(Q_i)$ without any apparent loss of accuracy [8]:

$$\phi(P) = \sum_i \frac{\sigma(Q_i)}{|P - Q_i|}, \tag{6}$$

and consequently, no numerical integration is needed, which greatly simplifies the solution process and reduces computational cost. Also, the role played by the elements is only marginal in the DIBIM (cf. the following discussions). Applying Equation (6) to Equations (3) and (4) gives rise to a system of equations from which the source density function $\sigma(Q_i)$ can be determined. After the source density distribution is found, the material velocity of the bubble can be obtained by direct differentiation of (6), which is another advantage of the current method. The indirect formulation hence obviates the need to compute an accurate normal of the surface, which is essential in direct boundary integral formulation in order to define the surface velocity. With the source points being moved away from the original boundary, the differentiation would not present any difficulty, as opposed to the conventional IBIM. After the velocity is found, the evolution of the bubble and ϕ according to Equations (1) and (2) is computed by a simple Eulerian scheme. This scheme has been used in most of the previous work on bubble dynamics [7,10,11], and therefore it is also adopted here in order to highlight the major difference between the current method and other methods. However, more sophisticated algorithms, such as the fourth-order Runge–Kutta method, may be worth trying in order to obtain more accurate results. It was also found that, unlike the axisymmetric problems, no artificial smoothing is necessary for the three-dimensional cases.

The desingularization actually results in a Fredholm integral equation of the first kind, and thus the desingularization distance must be carefully chosen to avoid ill-conditioning. As noted in Cao *et al.* [8], there exists an optimal distance that must be a function of the local mesh size. They proposed that this distance from a point P on the original boundary along the normal direction be represented by

$$L_{\mathrm{d}} = LD^{\alpha}, \tag{7}$$

where L is a parameter that reflects how far the integral equation is desingularized, D is the local mesh size, which is chosen here to be the square root of the averaged area of the triangular elements surrounding a vertex P, and α is a parameter that must be carefully chosen. Following Cao *et al.*, we fix α at 0.5 and try to find the optimal value for L from the simple example of the Rayleigh bubble.

With the buoyancy effect being neglected (i.e. $\delta = 0$) and the bubble being generated in an infinite fluid (i.e. there are no solid structures or free surface present), the bubble undergoes periodical expansion and contraction motion, which can be described by the Rayleigh–Plesset equation. In terms of the non-dimensional variable, the half period of the oscillation is about 0.915, at which the bubble attains its maximum radius. Figure 2 shows the errors of the computed bubble radius compared with the fourth-order Runge–Kutta solution of the Rayleigh–Plesset equation at $t = 0.915$ as a function of L. In this example, the bubble surface was discretized into 980 elements. The normal vector at a boundary point P was estimated as the weighted average of the normals to the triangular elements surrounding this point, with the weights being the inverse of the area of each element (since the smaller the area is, the closer the normal vector of this element is to the true normal at this point). Then the source points are placed at a distance given by Equation (7) from the corresponding boundary points along the estimated normal directions. It is worth remarking here that, unlike the calculation of

Copyright © 1999 John Wiley & Sons, Ltd.

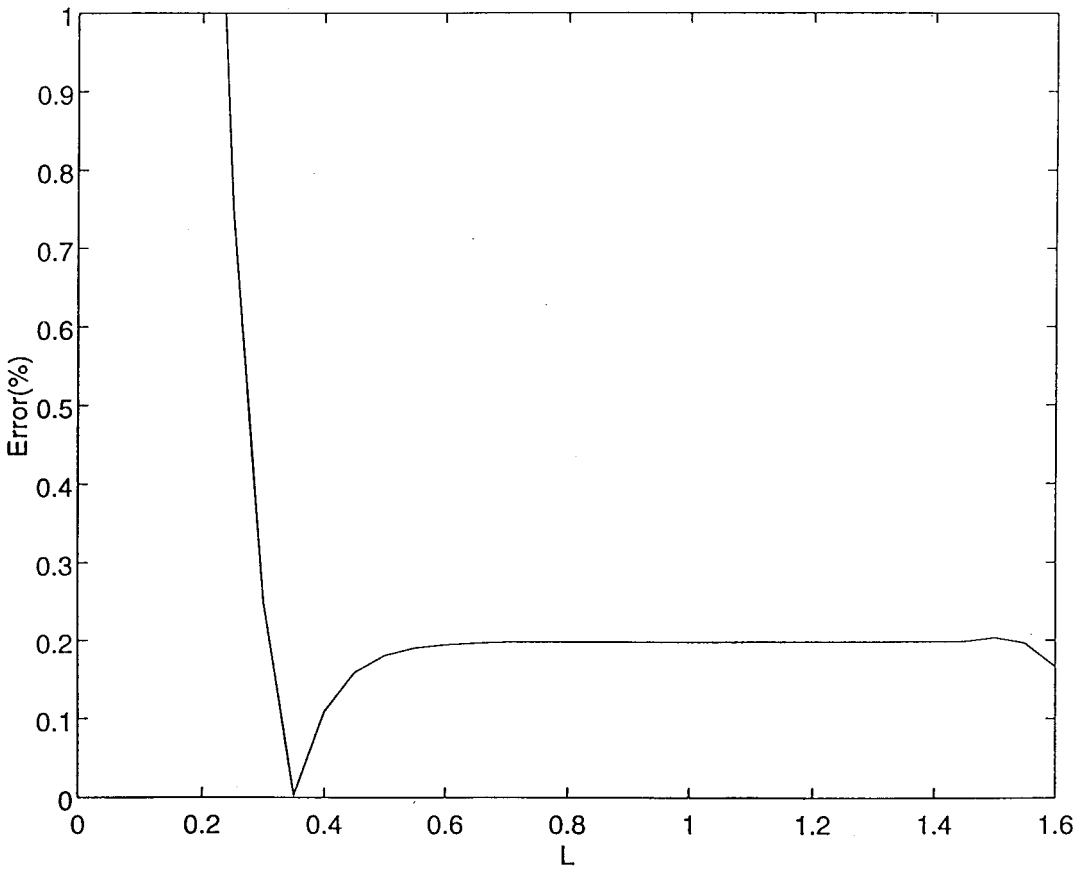

Figure 2. Numerical error as a function of the desingularization distance L.

normal and tangential vectors in the direct formulations, the accuracy of the estimated normal here is not essential since it only serves as a tool for placing the source points.

The trend shown in Figure 2 is very much similar to those shown in Figure 4 in Reference [8], with a sharp decline in the error near $L = 0$ and a broad range of L ($0.5 \leq L \leq 1.5$) in which the error is very small and insensitive to the variation of L. When L is slightly increased from 1.6, the computation stops prematurely at a rather early stage ($t = 0.04$) and the bubble fails to grow to its maximum size. In anticipation of the small bubble size at the end of the collapse phase, a smaller value of L is preferred. In this paper, we set $L = 0.5$.

3. RESULTS AND DISCUSSIONS

With the desingularization parameters having been fixed, we proceed to study various problems involving the interaction between bubbles and a solid wall. When a solid wall is placed below an initially spherical bubble, a jet directed towards the wall will be formed at the final stage of bubble collapse if the buoyancy effect is weak. Owing to the presence of the wall, we only need to modify the Green's function in Equation (6) to include the images of Q_i. In this case, a total number of 1280 elements were used in the discretization of the bubble. For

Copyright © 1999 John Wiley & Sons, Ltd.

the ease of presentation, only the bubble profiles at the end of the collapse phase, calculated from an axisymmetric model proposed by Wang *et al.* [11], the fully three-dimensional model based on the direct approach as proposed by the present authors [5] and the current model, are shown in Figure 3. The discrepancy between the axisymmetric code and the two three-dimensional codes is quite obvious, with a time lag of about $\Delta t = 0.03$ existing between them. The same was also noticed by the present authors when they proposed the robust three-dimensional model based on the nine-noded Lagrangian element in Reference [5]. For further comparative testing, the configuration was simulated where the initial distance between the bubble and the wall is substantially larger (ten maximum bubble radius). In this case, one would expect that the bubble motion should resemble that of a Rayleigh bubble, at least during the expansion phase, and thus the total expansion time should be very close to 0.915, the half-period of a Rayleigh bubble. The total expansion time calculated from the two three-dimensional models, which are based on quite different methodologies, is virtually indistinguishable from this value, but the time obtained from the axisymmetric code is still 3% larger than the above time. In the axisymmetric model of Wang *et al.* (as well as other axisymmetric models), artificial smoothing is indispensable in order to damp out the numerical instability, and this may have slowed down the bubble motion. On the other hand, no

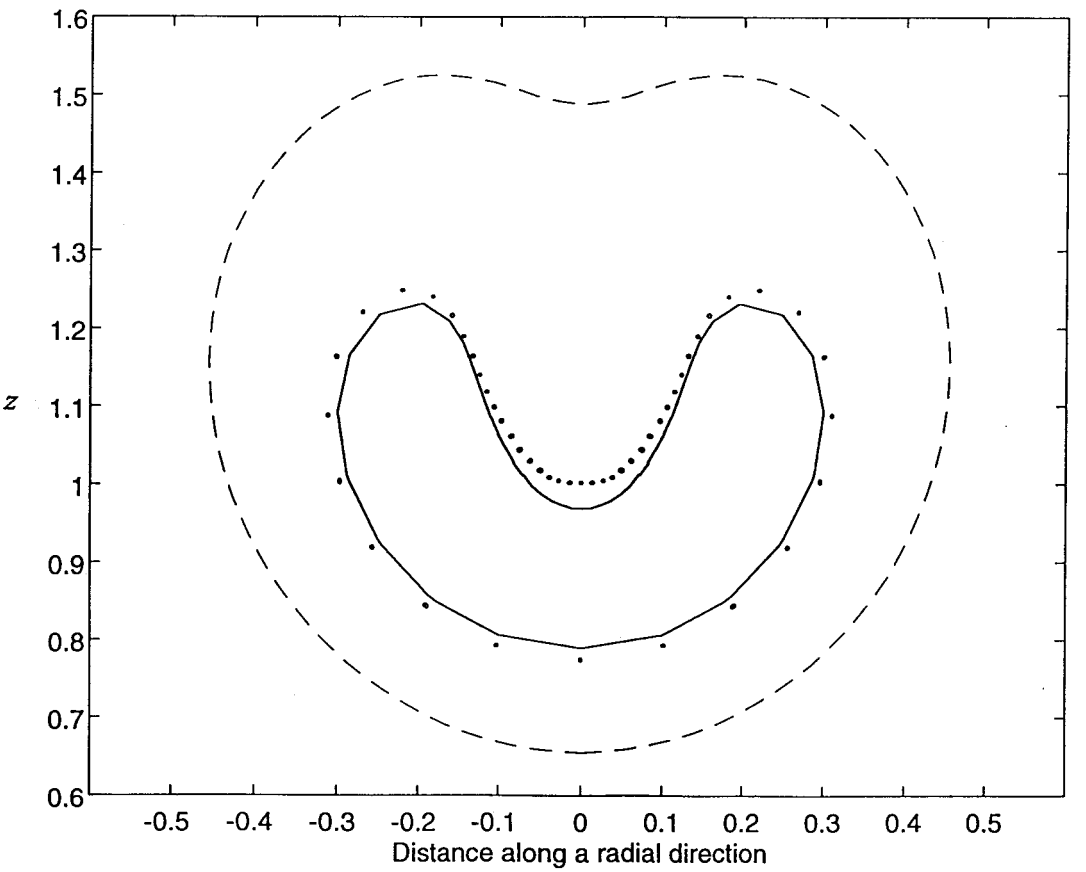

Figure 3. Comparison of the bubble profiles at $t = 2.014$, calculated from the axisymmetric model in [11] (dash line), the fully three-dimensional model in [5] (solid line) and the new model (dotted line). The initial distance between the bubble and the wall is 1.5 and the buoyancy effect is neglected ($\delta = 0$).

Copyright © 1999 John Wiley & Sons, Ltd.

smoothing is required in the two three-dimensional models. Hence, the two three-dimensional solutions, which agree very well with each other, are believed to be more accurate. As the re-entrant jet approaches the opposite bubble surface, the approaching nodal points (coming from opposite surfaces of the bubble) lead to an increasingly ill-conditioned matrix. An increasingly small time step is required to maintain computational stability. The development of the jet finally comes to a virtual halt. This effect is more severe in the case of the indirect method because the nodal points are located inside the bubble instead of on the bubble surface. Thus, the final computed time is $t = 2.019$ for the indirect method compared with $t = 2.026$ for the direct method. This problem can be partially overcome by switching back to the direct method at an appropriate point of time. With the indirect method, there is a handsome saving of 89% in the CPU time per time step.

A methodology for computing toroidal bubbles (where the jet needs to be as close to the opposite side of the bubble as possible so that a surgical cut can be made) is suggested as follows. One can use the desingularized indirect method to compute the evolution of the bubble until the jet comes close to the opposite wall of the bubble. One then switches to the direct method to compute the final phase of jetting and the formation of the toroidal bubble. The further evolution of the toroidal bubble is then computed by the indirect method. Significant gain in overall computational efficiency can be achieved in this manner.

As the re-entrant jet is being developed, more and more nodes are drawn from other parts of the bubble to the jet, where the curvature is highest, because of the Lagrangian method used [cf. Equations (1) and (2)]. As a result, the elements in other part of the bubble are stretched and this is ominous for the numerical accuracy and stability. Although no urgency for remeshing in the computations prior to the jet impact was found, it may become a major issue during and after the impact due to the expected large circulation around the bubble. Fortunately, remeshing is relatively easier with the present model because the elements only play a nominal role here.

Next, a fully three-dimensional bubble in the vicinity of a vertical wall is examined, where the combined effects of buoyancy and the Bjernes force have caused the bubble to evolve in a non-axisymmetric fashion. Of course, the axisymmetric code of Wang *et al.* [11] cannot be used in this case. The bubble is initiated at a non-dimensional distance of 1.5 from the wall. It can be seen from Figure 4 that the re-entrant jet during the collapse phase of the bubble ($t \geq 1.8859$) is essentially directed towards the wall but is diverted slightly upwards due to the buoyancy effects. The sequence of events in Figure 4(a) is computed using the direct model in [5]. In addition, the evolution of the bubble according to the DIBIM is shown next in Figure 4(b), while the results of Blake and Tong [12] are reproduced in Figure 4(c). It can be seen that the three solutions show similar behaviour for bubble growth and collapse, while the two three-dimensional models proposed by the present authors have predicted a slightly earlier jet formation compared to Blake and Tong's results. As is consistent with the previous example, the jet corresponding to the new indirect model is arrested earlier than those corresponding to the other two models. This is, however, more than amply compensated by 89% saving in the CPU time compared with the direct model. As proposed earlier, one can always use the indirect method for the initial computation for the purpose of computational efficiency before switching over to the direct method in the final jetting phase.

Finally, it should be remarked that the great saving in computational cost obtained by the current desingularized indirect model is achieved with a standard solver using the lower–upper (LU) decomposition method. For very large linear systems, such as those encountered in the present work, iterative methods will be more advantageous since the solution from the previous time step can be used as a good initial guess.

Copyright © 1999 John Wiley & Sons, Ltd.

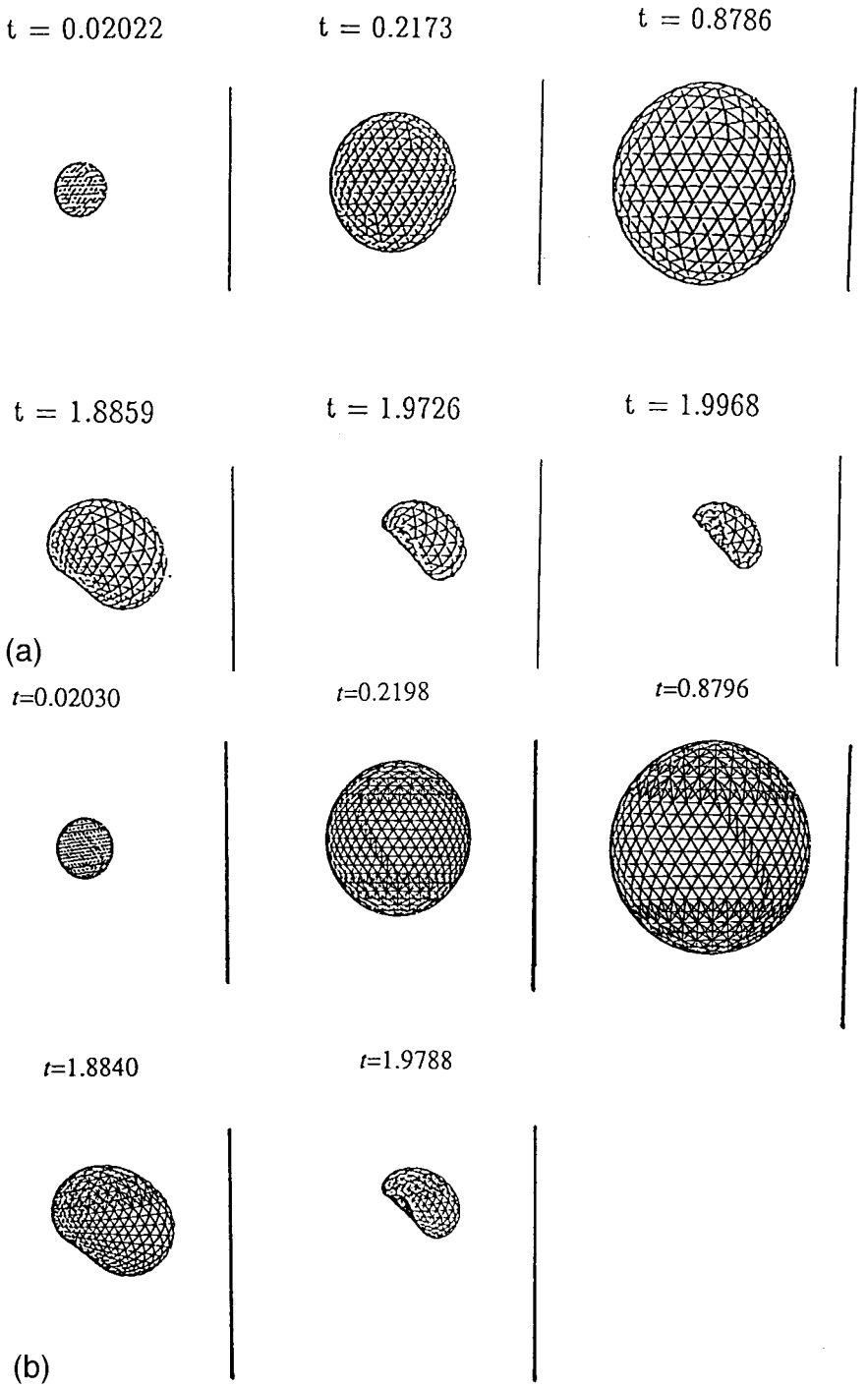

Figure 4. Evolution of a cavitation bubble near a vertical wall initially located at a distance 1.5 from the bubble centre. The buoyancy parameter $\delta = 0.25$. The results were calculated respectively from (a) the direct method in [5]; (b) the current indirect method; and (c) Blake and Tong's method [12]. The wall position is indicated by a vertical line in (a) and (b) and by the right-hand-side of the frame in (c).

Copyright © 1999 John Wiley & Sons, Ltd.

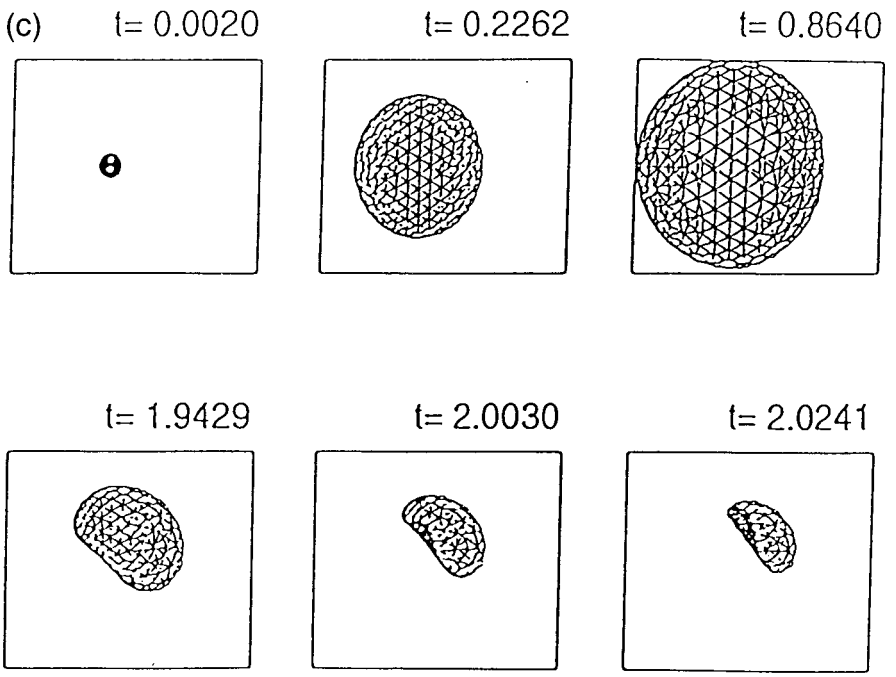

Figure 4 (*Continued*)

4. CONCLUDING REMARKS

In the present paper, a DIBIM is applied to the simulation of three-dimensional bubbles. With the desingularization parameters being carefully selected, it is shown that the results are in excellent agreement with those from the more complicated direct models proposed by others [3,4] and by the present authors [5]. The computational time and storage requirements are significantly reduced due to the simplicity of the new method, which is especially easy to apply when mesh refinement is required. Although with this model the time stepping tends to slow down as two surfaces approach each other, this can be easily rectified by switching over to a direct method so that the two surfaces can be drawn closer as required in the context of jet impact. After the impact process is completed, the new model can be reinstated to treat the complicated doubly connected geometry involving toroidal bubbles.

REFERENCES

1. C.A. Brebbia, J.C.F. Telles and L.C. Wrobel, *Boundary Element Techniques*, Springer, Berlin, 1984.
2. P.J. Harris, 'A numerical model for determining the motion of a bubble close to a fixed rigid structure in a fluid', *Int. J. Numer. Methods Eng.*, **33**, 1813–1822 (1992).
3. J.R. Blake, J.M. Boulton-Stone and R.P. Tong, 'Boundary integral methods for rising, bursting and collapsing bubbles', in H. Power (ed.), *BE Applications in Fluid Mechanics*, vol. 4, Computational Mechanics Publications, Southampton, 1995, pp. 31–72.
4. G.L. Chahine, T.O. Perdue and C.B. Tucker, 'Interaction between an underwater explosion bubble and a solid submerged body', *Tech. Rep. 86029-1*, Traycor Hydronautics, Inc., 1988.
5. Y.L. Zhang, K.S. Yeo, B.C. Khoo and W.K. Chong, 'Three-dimensional computation of bubbles near a free surface', *J. Compt. Phys.*, **146**, 105–123 (1998).
6. J.R. Blake and D.C. Gibson, 'Growth and collapse of a vapour cavity near a free surface', *J. Fluid Mech.*, **111**, 123–140 (1981).

Copyright © 1999 John Wiley & Sons, Ltd.

7. J.M. Boulton-Stone, 'A comparison of boundary integral methods for studying the motion of a two-dimensional bubble in an infinite fluid', *Comput. Methods Appl. Mech. Eng.*, **102**, 213–234 (1993).
8. Y. Cao, W.W. Schultz and R.F. Beck, 'Three-dimensional desingularized boundary integral methods for potential problems', *Int. J. Numer. Methods Fluids*, **12**, 785–803 (1991).
9. J.R. Blake, B.B. Taib and G. Doherty, 'Transient cavities near boundaries. Part 1. Rigid boundary', *J. Fluid Mech.*, **170**, 479–497 (1986).
10. J.P. Best, 'The dynamics of underwater explosions', *Ph.D. Thesis*, The University of Wollongong, Australia, 1991.
11. Q.X. Wang, K.S. Yeo, B.C. Khoo and K.Y. Lam, 'The evolution of a gas bubble in a shallow water', *12th Australian Fluid Mechanics Conference*, vol. 2, The University of Sydney, Sydney, 1995, pp. 823–826.
12. J.R. Blake and R.P. Tong, 'Jet impact in collapsing bubbles', *12th Australian Fluid Mechanics Conference*, vol. 2, The University of Sydney, Sydney, 1995, pp. 819–822.

Copyright © 1999 John Wiley & Sons, Ltd.